J Mater Sci (2007) 42:3739–3744
DOI 10.1007/s10853-006-0485-x

Effect of MgF_2 on hot pressed hydroxylapatite and monoclinic zirconia composites

Zafer Evis · Robert H. Doremus

Received: 2 September 2005 / Accepted: 1 June 2006 / Published online: 10 February 2007

Abstract Hydroxylapatite (HA) has been widely used in biomedical applications because of its excellent biocompatibility in the human body. A total of 25 wt% monoclinic (m) zirconia–HA composites (with and without 5 wt% MgF_2) were synthesized to investigate their mechanical properties and phase stability. In HA–m-ZrO_2 composites, HA and m-ZrO_2 reacted to form $CaZrO_3$ when there was no F^- present in the composite and m-ZrO_2 partially transformed to tetragonal ZrO_2. When MgF_2 was added into the system, it improved the thermal stability of the phases, densification, hardness, and fracture toughness of the composites and it caused the m-ZrO_2 to transform completely to t-ZrO_2 by incorporating the Mg^{2+} ions present in MgF_2 in the ZrO_2. Moreover, the stability of HA was improved by incorporating the F^- ions from MgF_2 in place of OH^- ions in HA. Substitution of OH^- by F^- ions was verified by the change in HA's hexagonal lattice parameters. A fracture toughness of 2.0 MPa$\sqrt{m}$ was calculated for the composite containing MgF_2.

Z. Evis
Engineering Sciences, Middle East Technical University, Ankara 06531, Turkey

R. H. Doremus (✉)
Materials Science and Engineering, Rensselaer Polytechnic Institute, 8th street, Troy, NY 12180, USA
e-mail: doremr@rpi.edu

Introduction

Hydroxylapatite (HA, $Ca_{10}(PO_4)_6(OH)_2$) is mainly used as a hard tissue implant because the inorganic part of the bone is composed of carbonated HA. Although it has excellent biocompatibility in the human body, a HA implant can only be used in non-load bearing areas i.e., in the middle ear [1]. To overcome the brittle nature of HA, composites of it with zirconia can be used to combine the advantages of the HA's biocompatibility and the high strength of zirconia.

When HA is sintered in air at temperatures ranging from 1,100 °C to 1,400 °C, HA decomposes and reacts to form unwanted second phases (i.e., α and β tri-calcium phosphate (TCP)) [2]. HA can be made more resistant to high temperature sintering by substituting impurity ions in its structure, such as Na^+, Mg^{2+}, Y^{3+}, CO_3^{2-}, F^- [3, 4].

HA–zirconia composites can be produced by mixing calcium–phosphate and zirconia powders, cold pressing and then sintering in different environments [5, 6]. Although pure HA starts to decompose to TCP at 1,300 °C, second phase formation starts well below 1,300 °C in the presence of ZrO_2 [2, 3, 6, 7]. Zirconia accelerates the decomposition of HA as seen in the reaction shown below [3]:

$$Ca_{10}(PO_4)_6(OH)_2 + ZrO_2(t) \xrightarrow{1{,}350^\circ C} 3\beta Ca_3(PO_4)_2 + ZrO_2(c)/CaZrO_3 + H_2O \quad (1)$$

Sinterability and mechanical properties of the 3 mol% Y_2O_3–ZrO_2 (up to 40 vol%)–HA composites was enhanced by increasing the green density of the

composites by cold isostatic pressing and the addition of small amounts of CaF_2 after the air sintering at 1,350 °C [3]. Fracture toughness (K_{1c}) of the HA–ZrO_2 composites (1.7–2.3 MPa$\sqrt{m}$) is higher than that of pure HA (1 MPa$\sqrt{m}$) [3, 8, 9].

In this study, the effects of MgF_2 on the HA–zirconia composites were examined the first time. A base composition of 75 wt% HA and 25 wt% ZrO_2 was chosen because previous work in our laboratory showed improved mechanical properties over pure HA with this composition (to be published). About 5 wt% of MgF_2 was added to some of the composites because a few % of fluoride suppresses the decomposition of HA by ZrO_2 at sintering temperatures [3]. HA and ZrO_2 powders were mixed by ball milling and hot pressed at 1,100 °C and 1,200 °C for 1 h. X-ray diffraction (XRD) was used to study the phase transformations in the composites. Vickers μ-hardness and the K_{1c} of the composites were measured. Scanning electron microscopy (SEM) was used to observe the grain size and the porosity in the composites.

Experimental procedure

The materials used in this research were pure HA synthesized with a precipitation method and composites of HA with monoclinic (m) zirconia made by hot pressing.

HA was synthesized by mixing solutions of calcium nitrate and di-ammonium hydrogen phosphate in the alkaline pH region [10]. First, 0.5 M calcium nitrate and 0.3 M di-ammonium hydrogen phosphate were prepared in distilled water separately. Ammonium hydroxide was added to both of these solutions to bring the pH level to 11–12. The calcium nitrate solution was added dropwise into the continuously stirred ammonium phosphate solution, producing a milky solution. After stirring the HA solution for 2–3 h, it was heated at 90 °C for 1 h during stirring to decrease the reaction time. Then, the HA solution was stirred for 1 day at room temperature. In the next step, the solution was washed repeatedly to remove the remaining ammonia and then filtered using a fine filter paper. The filtered wet cake was dried in an oven at 60–90 °C overnight to remove the excess water. Finally, the dried cake was air sintered at 1,100 °C to full density; it was heated and cooled in the furnace.

The powders of m-ZrO_2 (2 μm as an average particle size, Goodfellow, Cambridge, UK) were mixed with HA powder. First, dried HA particles were ground to—75 μm (–200 mesh) powder using a mortar and pestle. They were calcined at 900 °C for 1 h and then mixed with zirconia powders by ball milling with the zirconia balls in a porcelain container in ethyl alcohol for 24 h. Mixed powders were hot pressed at 1,100 °C and 1,200 °C using a high temperature–high vacuum furnace (Thermal Technology Inc., Concord, NH) under 60 MPa pressure.

All the samples were characterized by XRD with a Scintag Inc., XDS-2000 diffractometer with CuKα radiation at 50 kV/30 mA. Each sample was scanned from 20° to 50° in 2θ with a scanning speed of 1 degree/min. The hexagonal lattice parameters of HA were calculated by successive approximations [11].

The density of a hot pressed disc was calculated by dividing the weight by its volume. The theoretical density of the composites (components *a* and *b*) was calculated from the known weights *W* and densities ρ by the following formula.

$$\text{Density } (\text{gm}/\text{cm}^3) = \frac{W_a + W_b}{\left(\frac{W_a}{\rho_a} + \frac{W_b}{\rho_b}\right)} \tag{2}$$

Component "*a*" is ZrO_2 and component "*b*" is HA and TCP. The density of HA and of TCP was assumed to be the same for simplicity.

Micro (μ)-hardness of the hot pressed samples was measured with a Vickers μ-hardness tester with a diamond indenter at 200 gm (or 300 gm) load for 10 s. Approximately, 20 measurements were performed on each sample. The hardness value for each sample was calculated by:

$$\text{HV} = 0.001854 * \frac{P}{d^2} \tag{3}$$

where HV: Vickers hardness, *P*: Applied load, *d*: diagonal indent length.

K_{1c} of the composites was determined from cracks formed in the Vickers μ-hardness test. The Palmqvist equation for the K_{1c} of the composites is [12]:

$$K_{1c} = 0.035 * \left(\frac{H^{0.6} * E^{0.4}}{\phi^{0.6}}\right) * \left(\frac{a}{(c-a)^{0.5}}\right) \tag{4}$$

where, *H*: Hardness, *E*: Young's Modulus, ϕ: a dimensionless coefficient related to the material constraint ($\phi \cong 3$).

A JOEL (JSM-840) SEM at a voltage of 20 kV was used to examine the samples. Samples were etched with a 0.15 M lactic acid for 10 s and then rinsed in water and dried. They were coated with platinum under vacuum before characterization in SEM.

Results

XRD results of sintered HA's are presented in Fig. 1. XRD peaks for the 1,100 °C sintered HA are very sharp and narrow. This shows that HA grains were larger than about 0.1 μm and highly crystalline after sintering. Air sintering of precipitated pure HA at 1,100 °C for 1 h resulted in a fully dense material, which had an average Vickers μ-hardness of 4.7 ± 0.35 GPa and a K_{1c} of 0.95 ± 0.05 MPa√m.

ZrO_2 (as received) had a monoclinic structure with a negligible amount of tetragonal (t) ZrO_2 phase, as seen in Fig. 2d. When the m-ZrO_2 powders were sintered at 1,100 °C for 1 h, no phase change in the m-ZrO_2 was observed (Fig. 2e).

Starting green densities of the composites were about 54% of the theoretical density for the HA–m-ZrO_2 composites. Densification of the 25 wt% m-ZrO_2–HA (with and without 5 wt% MgF_2) composites was decreased when the sintering temperature increased from 1,100 °C to 1,300 °C as shown in Fig. 3.

XRD results of HA–m-ZrO_2 composites with and without 5 wt% MgF_2, which were sintered at 1,100 °C and 1,200 °C, are presented in Fig. 4. Although m-ZrO_2 did not transform to t-ZrO_2 when it was sintered at 1,100 °C as a monolithic phase (Fig. 2e), m-ZrO_2 partially transformed to t-ZrO_2 in the composites after sintering at 1,100 °C and 1,200 °C because of the presence of HA (Fig. 4). Ca^{2+} ions in HA caused the m-ZrO_2 to partially transform to the tetragonal phase by the transfer of Ca^{2+} from HA into ZrO_2. Therefore,

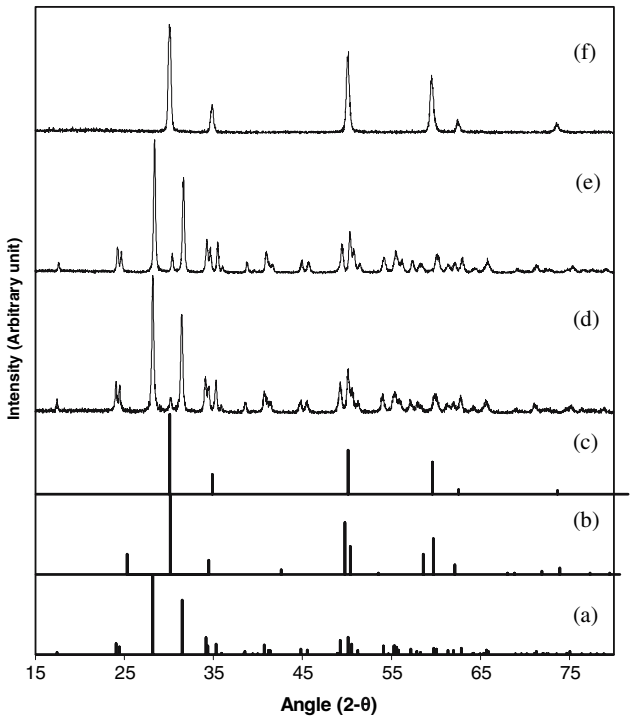

Fig. 2 XRD spectra of zirconias: (**a**) m-ZrO_2 (JCPDS # 37-1484); (**b**) t-ZrO_2 (JCPDS # 17-0923); (**c**) c-ZrO_2, 8% Y_2O_3 (JCPDS # 30-1468); (**d**) Pure ZrO_2 as received, (**e**) ZrO_2, sintered at 1,100 °C for 1 h; (**f**) ZrO_2, 8% Y_2O_3

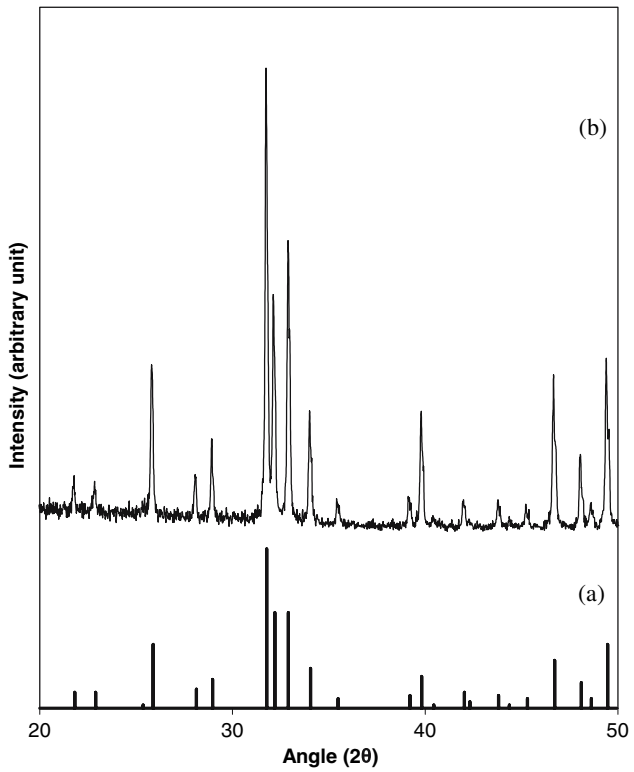

Fig. 1 XRD spectra of standard HA (JCPDS # 9-432) (**a**) and HA sintered at 1,100 °C for 1 h (**b**)

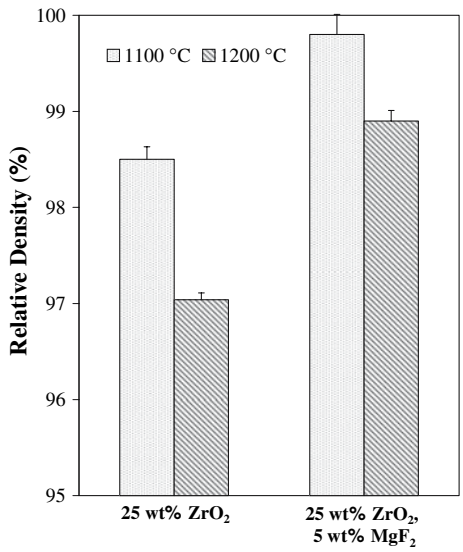

Fig. 3 Relative density of the composites after the sintering at 1,100 °C and 1,200 °C

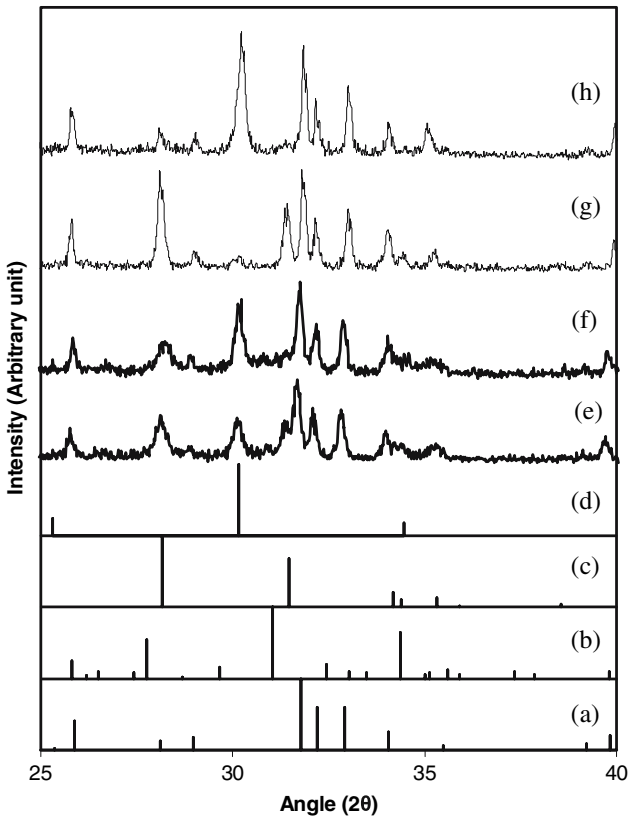

Fig. 4 XRD spectra of the hot pressed composites: (**a**) HA (JCPDS # 9-432); (**b**) β-TCP (JCPDS # 9-169); (**c**) m-ZrO_2 (JCPDS # 37-1484); (**d**) t-ZrO_2 (JCPDS # 17-0923); (**e**) 25 wt% m-ZrO_2, 1,100 °C for 1 h; (**f**) 25 wt% m-ZrO_2, 1,200 °C for 1 h; (**g**) 25 wt% m-ZrO_2, 5 wt% MgF_2, 1,100 °C for1 h; (**h**) 25 wt% m-ZrO_2, 5 wt% MgF_2, 1,200 °C for 1 h

small amounts of β-TCP and α-TCP were observed at 1,100 °C and 1,200 °C, and OH^- ions were also removed from the HA because of its decomposition at high temperatures in the presence of ZrO_2. From the comparison of the m-ZrO_2 and t-ZrO_2 XRD peak heights, the amount of phase transformation increased when the sintering temperature increased from 1,100 °C to 1,200 °C. A small amount of $CaZrO_3$ formed in all composites. Although there was no transformation from m-ZrO_2 to t-ZrO_2 when the 5 wt% MgF_2–25 wt% m-ZrO_2 composite was sintered at 1,100 °C (Fig. 4g), a complete transformation from m-ZrO_2 to t-ZrO_2 was observed for the same composite after sintering at 1,200 °C (Fig. 4h).

The lattice parameters of the HA that remained in the composites after the reactions are presented in Table 1. The lattice parameters and hexagonal unit cell volume of HA increased from those of pure monolithic HA when there was only HA and m-ZrO_2 present in the composites. When there was MgF_2 present in the composites, the unit volume of the HA decreased because of the substution of OH^- ions by F^- ions.

Vickers μ-hardness results of the 25 wt% m-ZrO_2–HA composites are presented in Fig. 5. The μ-hardness of the composites decreased when the sintering temperature was increased from 1,100 °C to 1,200 °C. Porosity in the composites is presented in Fig. 3. There was porosity up to 3% in the composites after the sintering temperatures of 1,100 °C and 1,200 °C. High porosity in the composites resulted in poor μ-hardness. SEM micrographs of the composites sintered at 1,100 °C are shown in Fig. 6; the MgF_2 doped HA–zirconia composite was denser than the composite without MgF_2. Because of the difference in thermal expansion coefficients of HA and m-ZrO_2, cracks often formed along grain boundaries. Composites with 5 wt% MgF_2 resulted in higher hardness and gave the highest K_{1c} after hot pressing at 1,200 °C, as presented in Fig. 7. Increasing the sintering temperature from 1,100 °C to 1,200 °C decreased the K_{1c} of the composites.

Discussion

At temperatures above about 1,150 °C in ambient atmosphere, HA begins to decompose by the following reaction:

$$Ca_{10}(PO_4)_6(OH)_2 \rightarrow 3Ca_3(PO_4)_2 + CaO + H_2O \quad (5)$$

Zirconia in HA composites without added fluoride catalyzes this decomposition of HA. One reason for this catalysis is that the CaO formed in reaction 5 can react with the zirconia to form $CaZrO_3$:

$$CaO + ZrO_2 \rightarrow CaZrO_3 \quad (6)$$

We found X-ray evidence for $CaZrO_3$ in the sintered HA–ZrO_2 composites. Removal of the CaO from the reaction mixture then drives Eq. 5 to further decomposition of the HA.

Another process that removes CaO from the reaction mixture is dissolution of CaO in tetragonal ZrO_2. The original monoclinic ZrO_2 transforms to the tetragonal phase as CaO dissolves in it; the tetragonal phase has a distorted fluorite structure, in which oxides such as CaO, MgO, and Y_2O_3 show considerable solid solubility. Our X-ray results showed that some of the monoclinic ZrO_2 transformed to the tetragonal phase after sintering of the composites.

The addition of MgF_2 to the powder mixtures strongly reduced the tendency of the HA to decompose

Table 1 Lattice parameters of HA present in the m-ZrO_2 composites

ID	Hot pressing temp (°C)	Hexagonal lattice parameters of HA					
		a (Å)	Δa (Å)	c (Å)	Δc (Å)	V (Å^3)	ΔV (Å^3)
HA (JCPDS# 9-432)		9,427	0.000	6,889	0.000	1584.9	0.0
FA (JCPDS# 15-876)		9,372	–0.055	6,890	0.001	1566.8	–18.1
25 wt% ZrO_2	1,100	9,451	0.024	6,909	0.020	1597.7	12.8
25 wt% ZrO_2	1,200	9,440	0.013	6,892	0.003	1590.1	5.2
25 wt% ZrO_2, 5 wt% MgF_2	1,100	9,401	–0.026	6,907	0.018	1580.2	–4.7
25 wt% ZrO_2, 5 wt% MgF_2	1,200	9,393	–0.034	6,910	0.021	1578.3	–6.6

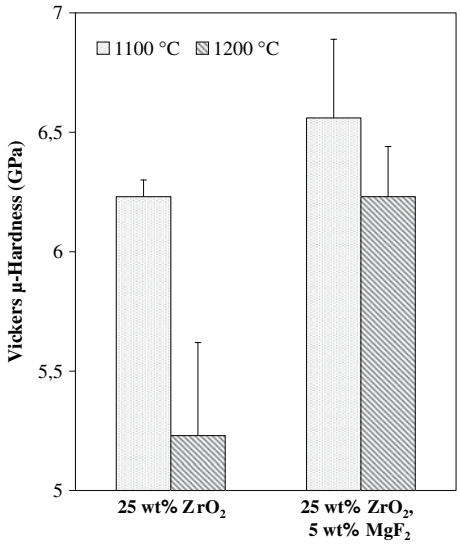

Fig. 5 Vickers μ-hardness of the composites sintered at 1,100 °C and 1,200 °C

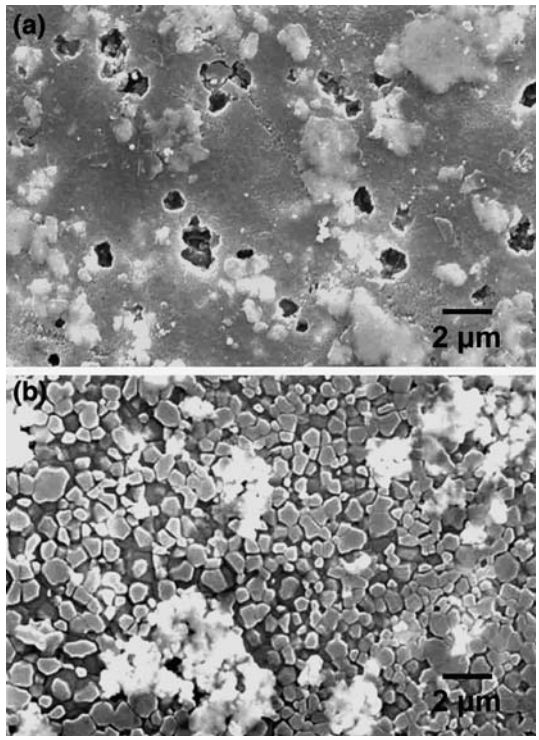

Fig. 6 SEM micrographs of the composites sintered at 1,100 °C: (**a**) 25 wt% ZrO_2 and (**b**) 25 wt% ZrO_2 with 5 wt% MgF_2

during sintering. We suggest that this reduction results because of substitution F^- ions for OH^- ions in the apatite structure [13–16]. The substitution reaction can be written as:

$$Ca_{10}(PO_4)_6(OH)_2 + MgF_2 \rightarrow Ca_{10}(PO_4)_6F_2 + MgO + H_2O \quad (7)$$

This reaction takes place at temperatures below the sintering temperatures of 1,100 °C and 1,200 °C [16]. Thus, the water formed in the reaction vaporizes from the powder mixture, driving reaction 7 to the right and the formation of fluorapatite.

The OH^- ions in the apatite structure are located in cavities parallel to the *c*-axis [13, 14]. They have an ionic radius greater than that of the fluoride ions, so substitution of F^- for OH^- ions leads to a contraction of the unit cell of the HA [13, 15]. Consistent with this contraction we found a decrease in the lattice parameters of HA in the composites with MgF_2 addition, as shown in Table 1.

Fluorapatite is more stable to decomposition at high temperatures than HA, consistent with the reduction of decomposition of HA after substitution of some fluoride ions for hydroxyl ions.

The suppression of the decomposition of the HA by addition of MgF_2 to the sintering powders led to lower porosity in the sintered material because less water was produced during sintering. This reduced porosity led to higher strength, hardness, and K_{1c} of the sintered composites.

Conclusion

Porosity in sintered HA–ZrO_2 composites was reduced by addition of 5% MgF_2 to the green powder mixture.

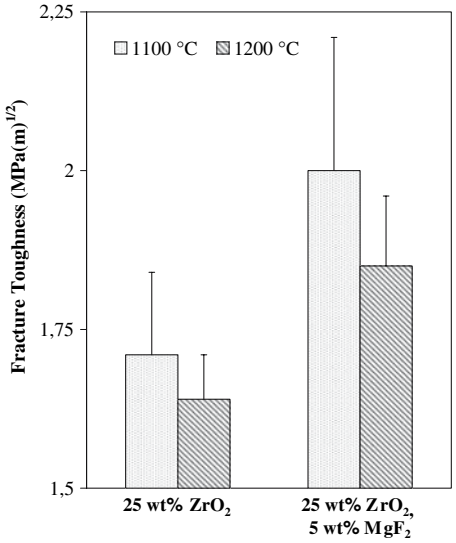

Fig. 7 Fracture toughness of the composites sintered at 1,100 °C and 1,200 °C

ZrO_2 alone catalyzed the high temperature decomposition of HA, leading to higher porosity; the substitution of F^- ions from the MgF_2 for OH^- ions in the HA structure suppressed the decomposition of HA, resulting in lower porosity of the sintered composites and higher strength, hardness and K_{1c} values.

References

1. Legeros RZ, Legeros JP (1993) In: Hench LL, Wilson J (eds) An introduction to bioceramics. World Scientific Publishing Co., Singapore, p 139
2. Matsuno T, Watanabe K, Ono K, Koishi M (1998) J Mater Sci Lett 17:1349
3. Kim HW, Noh YJ, Koh YH, Kim HE, Kim HM (2002) Biomaterials 23(20):4113
4. Kijkowska R, Lin S, Legeros RZ (2002) In: Brown S, Clarke I, Williams P (eds) Bioceramics, vol 14. Trans Tech Publications Ltd, Switzerland, p 31
5. Heimann RB, Vu TA (1997) J Mater Sci Lett 16:437
6. Rao RR, Kannan TS (2002) Mater Sci Eng C 20:187
7. Chang E, Chang WJ, Wang BC, Yang CY (1997) J Mater Sci Mater Med 8:193
8. Ahn ES, Gleason NJ, Nakahira A, Ying JY (2001) Nano Lett 1(3):149
9. Delgado JA, Morejon L, Martinez S, Ginebra MP, Carlsson N, Fernandez E, Planell JA, Clavaguera-mora MT, Rodriguez-Viejo J (1999) J Mater Sci Mater Med 10:715
10. Jarcho M, Bolen CH, Thomas MB, Babock J, Kay JF, Doremus RH (1976) J Mater Sci 11:2027
11. Cullity BD (1978) Elements of X-ray diffraction, 2nd edn. Addison-Wesley Publishing Company, Reading, MA, p 501
12. Slosarczyk A, Bialoskorski J (1998) J Mater Sci Mater Med 9:103
13. Narasaraju TSB, Phebe DE (1996) J Mater Sci 31:1
14. Kay MI, Young RA, Posner RS (1964) Nature 204:1050
15. Young RA (1974) J Dental Res 53:193
16. Elliott JC (1994) Structure and chemistry of the apatites and other calcium orthophosphates. Elsevier, NY, 161 pp